Available online at www.sciencedirect.com

ScienceDirect

Procedia Structural Integrity 2 (2016) 673–680

Structural Integrity Procedia

www.elsevier.com/locate/procedia

21st European Conference on Fracture, ECF21, 20-24 June 2016, Catania, Italy

Investigations of ductile damage in DP600 and DC04 deep drawing steel sheets during punching

Kerim Isik[a,*], Gregory Gerstein[b], Florian Gutknecht[a], Till Clausmeyer[a], Florian Nürnberger[b], Hans Jürgen Maier[b], A. Erman Tekkaya[a]

[a]*Institute of Forming Technology and Lightweight Construction, Technical University of Dortmund, Baroper Str. 303, 44227 Dortmund, Germany*

[b]*Institut für Werkstoffkunde (Materials Science), Leibniz Universität Hannover, An der Universität 2, 30823 Garbsen, Germany*

Abstract

The paper presents numerical and microstructural investigations on a punching process of 2 mm thick steel sheets. The dual phase steel DP600 and the mild steel DC04 exhibit different damage and fracture characteristics. To distinguish the void development and crack initiation for both materials, interrupted tests at varied punch displacements are analyzed. The void volume fractions in the shearing zone are identified by scanning electron microscopy (SEM). The Gurson model family, which is recently extended for shear fracture, is utilized to model the elastoplastic behavior with ductile damage. The effect of the shear governing void growth parameter, introduced by Nahshon and Hutchinson (2008), is discussed.

Peer-review under responsibility of the Scientific Committee of ECF21.

Keywords: Punching; Gurson model; dual phase steel; mild steel; shear fracture; SEM

1. Introduction

Sheet metal cutting operations such as blanking, fine blanking, trimming, guillotining and punching aim to separate a certain amount of the material from the remaining sheet by using a controlled shearing and fracture at the contour of cut. The properties of the resulting surface of cut depend on the proportion of the sheared and fractured regions. To this proportion, plastic flow, friction and fracture contribute simultaneously (Atkins, 1981). Material properties and process parameters such as sheet thickness, clearance, punch and die radii etc. define the cut surface properties.

* Corresponding author. Tel.: +49-231-755-6918; fax: +49-231-755-2489.
E-mail address: Kerim.Isik@iul.tu-dortmund.de

Peer review under responsibility of the Scientific Committee of ECF21.
10.1016/j.prostr.2016.06.087

For the process design, predictions of the surface characteristics and force requirements are mandatory. Analytical models provide acceptable estimations of the fraction of the sheared region and the maximal shearing force required for the cutting operations, cf. (Atkins, 1980) and (Martins and Atkins, 2013). Numerical modelling of the metal cutting processes using fracture models aims to improve predictions of the same manner as in (Thipprakmas et al., 2008). Hambli (2001) used the Lemaitre damage model (Lemaitre, 1985) and Rachik et al. (2003) applied the Gurson-Tvergard-Needleman (GTN) model (Tvergaard and Needleman, 1984) to simulate the fine blanking and the blanking process, respectively. Using those models, the fracture is mainly performed by removal of those elements, at which the damage has reached a critical threshold value. Main challenges in the numerical models are the requirement of very fine discretization (small mesh size) at the cutting zones and the occurrence of large deformations during the cutting process which follows excessive deformation of finite elements. To remedy those problems, Brokken et al. (1998) applied the Arbitrary-Lagrangian-Eulerian (ALE) method combined with remeshing. For the fractured region, Komori (2014) suggested a node-separation-method instead of element deletion to model fracture.

In this paper, the punching process is modelled using the Gurson model (Tvergaard and Needleman, 1984) which is recently extended for shear fracture (Nahshon and Hutchinson, 2008). In the Gurson model family, the material deterioration is measured by the void volume fraction f. The amount of voids, which may already be included at the initial state, is denoted by the initial void volume fraction f_0. During the deformation, nucleation of new voids and growth of already existing ones decreases the load carrying capacity of the material. Unlike Gurson's original model, which does not account for void evolution under shear stress, the modification in (Nahshon and Hutchinson, 2008) takes additional phenomenological effects of void distortion and void interactions with material rotation into consideration. The threshold values f_c and f_f define the onset of the coalescence and final fracture, respectively. The aim of this investigation is to prove the applicability of this model for a punching process, in which the shear stress states are dominant. A combined experimental and numerical investigation on the void evolution and succeeding fracture of two different sheet materials, namely a dual phase steel DP600 and a mild steel DC04 with the same sheet thickness of 2 mm is conducted. Specimens from interrupted tests at varied levels of punch displacements are used to measure voidage under scanning electron microscope at the intermediate stage of the punching process.

2. Gurson porous plasticity

The Gurson's yield function in general is (Gurson, 1977):

$$\Phi^P = \left(\frac{\sigma_{eq}}{\sigma_y}\right)^2 + 2q_1 f^* \cosh\left[\frac{3}{2}\frac{q_2\sigma_m}{\sigma_y}\right] - (1 - q_3 f^{*2}) = 0 \tag{1}$$

where σ_{eq} is the equivalent stress of von Mises, $\sigma_m = tr[\mathbf{T}]$ with $\mathbf{T}$ denoting the Cauchy stress tensor. q_1, q_2 und q_3 are material parameters (Tvergaard, 1981; Tvergaard, 1982). $\sigma_y = \sigma_y\,[e^p]$ is the flow stress and for the Swift type isotropic hardening with material parameters K, e_0 und n, it reads:

$$\sigma_y[e^p] = K\,(e_0 + e^p)^n \tag{2}$$

The volume void fraction is modified to f^*, due to the accelerating effects of the void coalescence as follows (Tvergaard and Needleman, 1984):

$$f^* = \begin{cases} f & f \le f_c \\ f_c + \dfrac{f_u^* - f_c}{f_f - f_c}\left(f - f_c\right) & f > f_c \end{cases} \tag{3}$$

where critical void volume fraction at incipient coalescence and the void volume fraction at final fracture are denoted by f_c und f_f, respectively. $f_u^*=1/q_1$ is the maximal value of the f^* at which the stress carrying capacity vanishes macroscopically. This corresponds to the trigger for the element deletion to model fracture.

Associative plastic flow is assumed using the normality rule:

$$\mathbf{d}^P = \dot{\gamma}\partial_{\mathbf{T}}\Phi^P \tag{4}$$

where $\mathbf{d}^P$ and $\dot{\gamma}$ are the plastic rate of deformation tensor and the plastic multiplier respectively.

The change in the void volume fraction $\partial_t f$ has contributions due to the nucleation of the new voids $\partial_t f^n$, void growth due to hydrostatic stresses $\partial_t f^g{}_{hyd}$ and void growth due to the shear stresses $\partial_t f^g{}_{shr}$:

$$\partial_t f = \partial_t f^n + \partial_t f^g_{hyd} + \partial_t f^g_{shr} \tag{5}$$

The void growth due to shear stress is (Nahshon and Hutchinson, 2008):

$$\partial_t f^g_{shr} = k_w f \frac{w\left(\mathrm{dev}\left[\mathbf{T}\right]\right)}{\sigma_{eq}} \mathrm{dev}\left[\mathbf{T}\right] : \mathbf{d}^p \tag{6}$$

Here, k_w is a material parameter and $w(\mathrm{dev}[\mathbf{T}])$ is a stress dependent function depending on the third invariant of the deviatoric stress tensor J_3 as follows:

$$w\left(\mathrm{dev}\left[\mathbf{T}\right]\right) = 1 - \left(\frac{27 J_3}{2\sigma_{eq}^3}\right)^2 \tag{7}$$

For further details of the model regarding to nucleation of the voids and the growth due to hydrostatic stresses, model implementation and related model parameters refer to (Soyarslan et al., 2011).

3. Punching experiments

3.1. Materials

Two sheet materials from different classes of steel are selected, namely DC04 and DP600 with sheet thicknesses of 2 mm. The elastoplastic material parameters are listed in Table 1.

Table 1. Mechanical properties of the materials

Steel	Modulus of Elasticity [MPa]	Poisson's ratio	Yield strength [MPa]	Swift hardening (Eq. 2)		
				K [MPa]	e_0	n
DC04	214000	0.3	165	619	0.00939	0.296
DP600	201400	0.3	359	983	0.00232	0.190

The Gurson model parameters related to initial voidage, void nucleation and growth are listed in Table 2. Those are identified using micromechanical investigations. For further details regarding to material characterization refer to (Soyarslan et al., 2011) and (Isik et al., 2016).

Table 2. Gurson model parameters for the materials

Steel	f_0	q_1	q_2	q_3	f_N	s_N	$e^p{}_N$	f_c	f_f
DC04	0.000269	1.5	1.0	2.25	0.003273	0.1	0.03	0.15	0.25
DP600	0.008	1.5	1.0	2.25	0.00062	0.1283	0.5421	0.15	0.25

3.2. Experimental setup

The experiments are conducted with a punching module that can be attached to universal testing machines with connection plates (Fig. 3). During the test, the punch force and displacement are recorded. The punch and die tip radii are 25 µm. The cutting clearance is 80 µm, which corresponds 4% of sheet thickness (2 mm). Punch radius is 8 mm. Further geometrical details are depicted in Fig. 3. In addition to the throughout punching tests, 6 interrupted tests are conducted to investigate the void and crack evolution during intermediate stages of the test.

3.3. Micromechanical investigations

Morphological comparison is done on the shearing zone of the specimens. The regions subjected to shearing followed by tearing can be distinguished by the shiny shear surface and the rough crack surface. For DC04 this regions have almost the same proportion. For DP600 a secondary shear surface is observed. After first shearing and a certain amount of tearing formation of a secondary shear surface is observed (Fig. 1). The total amount of the shear surfaces is 25% of the total surface.

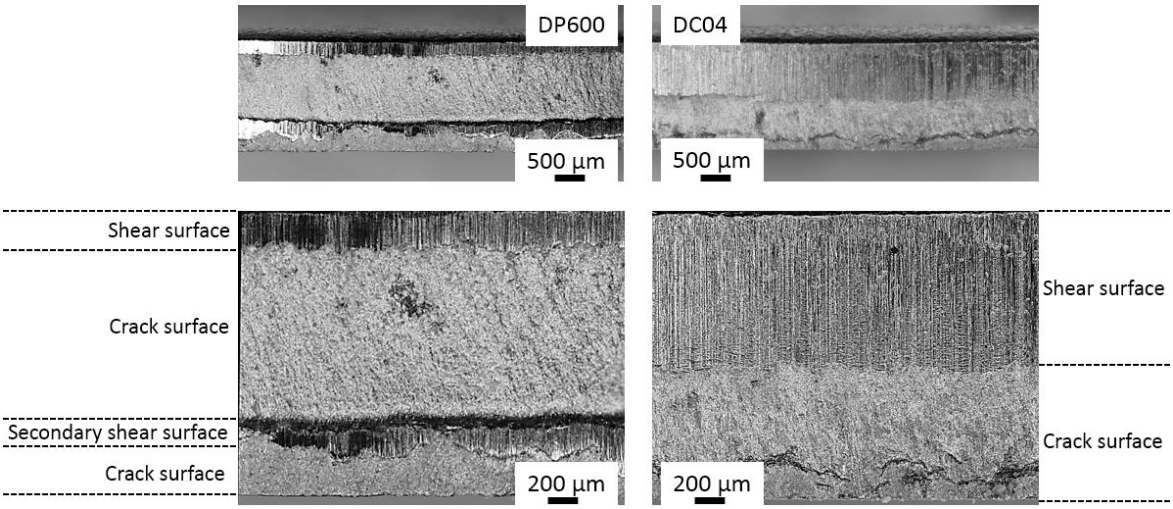

Fig. 1. Surface at cutting region

The specimens from interrupted tests are cut as shown in Fig. 2 in order to determine the critical punch displacement for the initiation of the macro-crack. The specimen, at which the crack initiated for DP600, is analyzed under SEM to measure the void volume fractions through thickness. This specimen is compared with the DC04 specimen, which has the same punch displacement. The cross section from the contact surface with punch to the crack tip is divided into 7 zones. For each zone, 5x5=25 regions are examined for the void fraction determinations. Each region has an area of 111 µm x 79.3 µm. Digital Image Correlation software is used to distinguish the voids from the matrix material and to measure the cross section area of the voids. Further details of the methodology are given in (Gerstein et al., 2016).

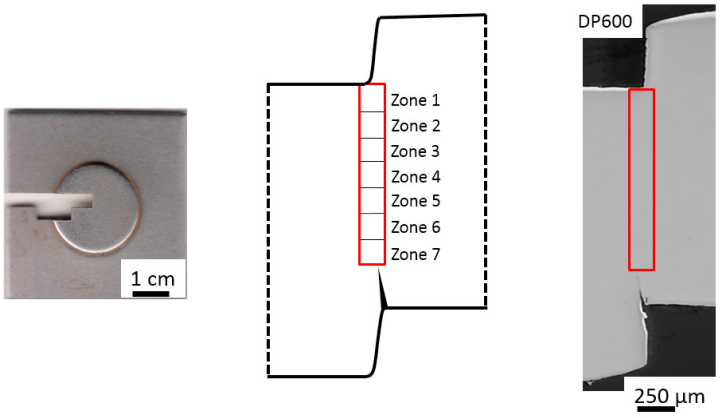

Fig. 2. Specimen cut for SEM analysis and zones at the cross section

3.4. Numerical model of the experiments

The Gurson model featuring shear extension as proposed by Nahshon and Hutchinson (2008), was implemented in Abaqus as a user defined subroutine VUMAT. The punching process was simulated using a two-dimensional axisymmetric model with CAX4R elements (4-node bilinear axisymmetric quadrilateral element) using Abaqus/Explicit. Fig. 3. depicts the details of the geometrical model. The mesh size at the cutting zone is 25 µm and constant at the fine meshed region of 1.5 mm length, which is reasonable for a punch tip radius of 25 µm and a cutting clearance of 80 µm. In order to eliminate the problem of excessive element distortion due to large deformations at the shearing zone, an Arbitrary-Lagrangian-Eulerian (ALE) mesh is applied. The crack is represented by the deletion of those elements, at which the void volume fraction reaches the critical value f_f. Punch and die are modelled as rigid bodies.

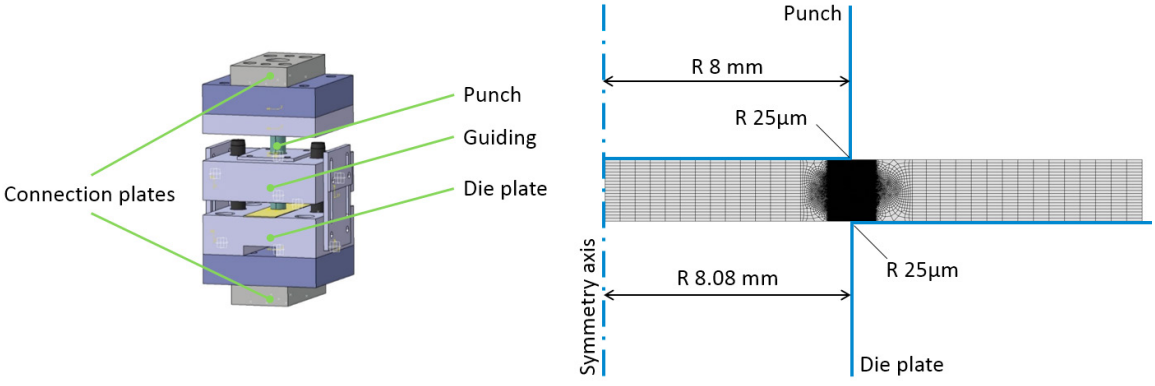

Fig. 3. Experimental setup and simulation model

4. Results

Punch force-displacement curves from the experiments are used to determine model parameter related to the void growth due to shear k_w (Eq. 6). For the case k_w=0, there is no contribution of the void growth due to shear stresses in the GTN model. That postpones the overall separation of the material at the cutting zone as seen in Fig. 4. For both materials, k_w=1 can predict the force response from the tests. For DP600, after the first force-drop of around 25% of the maximum force till punch displacement of 0.8 mm, the force decreases gradually till separation. The occurrence and existence of a secondary shear surface observed in the experiments, which maintains contact at the shearing zone, may cause this gradual decrease instead of a rapid drop of the force during cutting.

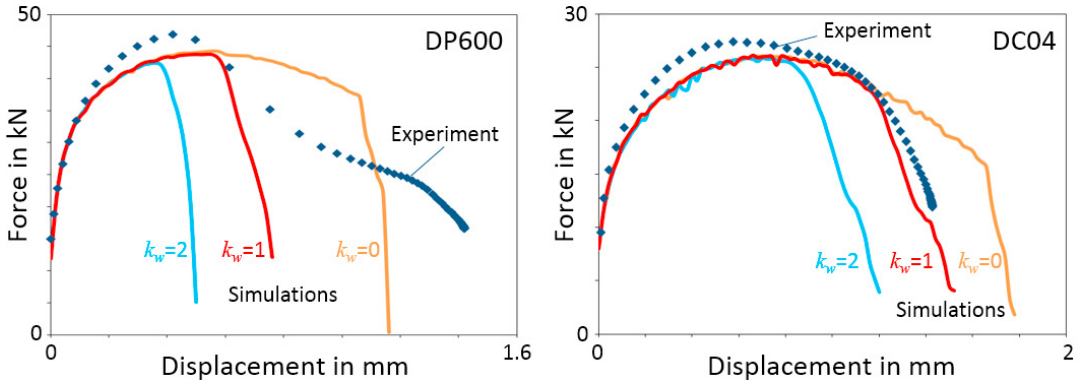

Fig. 4. Comparison of punch force-displacement for experiment and simulations with k_w=0, 1 and 2

In the following, cross sections at the shearing zone of experiments and simulations are compared for the selected shear parameter k_w=1. For both DP600 and DC04, a macro-crack is observed at a punch displacement of 0.70 mm and 0.95 mm, respectively. Regarding DP600, a secondary crack initiates from the punch side at a punch displacement of 1.20 mm. Those results are matching with the simulation results summarized in Fig. 5. Relatively late crack initiation for DC04 (at 1.20 mm punch displacement) compared to DP600 (at a punch displacement of 0.64 mm) occurs in the simulation results. Around 0.80 mm punch displacement, secondary cracking is observable at the simulation, which opens from the punch side. For DC04, the crack opens only from one side (contact region with die) of the specimen, as in the experiment.

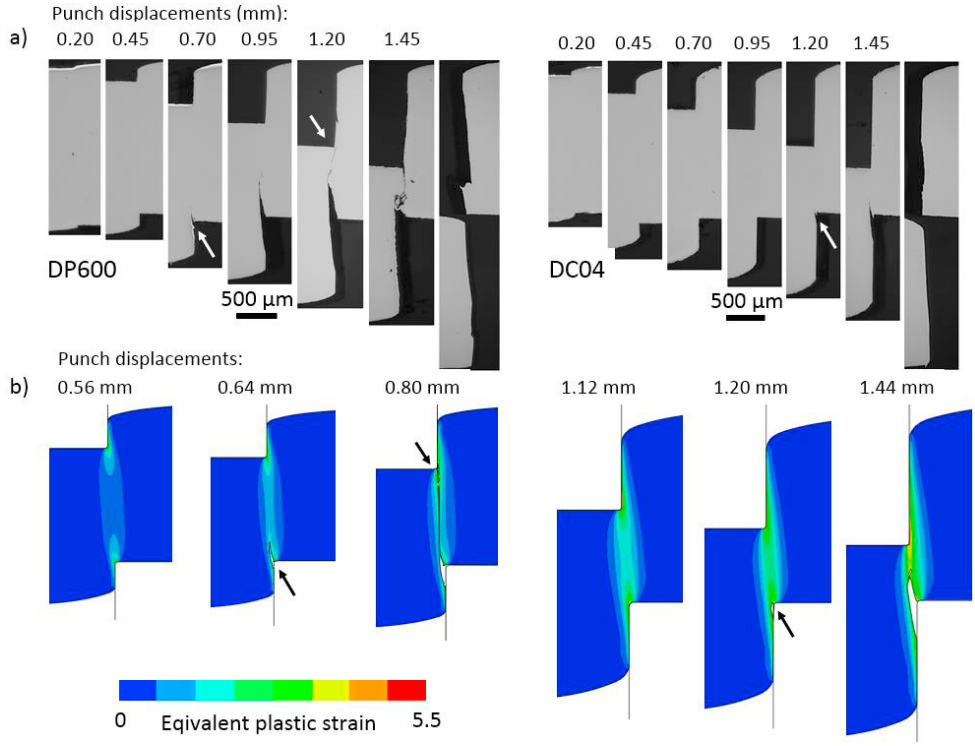

Fig. 5. Comparison of SEM results with simulations (k_w=1) (a) Cross sections from interrupted tests (b) Equivalent plastic strain at the cutting zone.

The shearing zone is investigated regarding the void volume fractions at the punch displacement of 0.70 mm. This corresponds to the initiation of cracking for DP600. At this punch displacement, the crack has not been observed at DC04 yet. In order to consider void events until the occurrence of a macro-crack, the crack region is excluded for the void measurement (Fig. 6). The void volume fraction for the specimens shows similar tendency for both materials; the minimum void volume fractions are observed at the mid of the cross section around zone 2 and 3. The maximum value is observed in zone 7 at the open side of punched part, at which the first crack opens. In zone 1, which is the closest one to the punch, the voidage is slightly higher than the minimum values. For DC04 this increase in the voids is marginal. This agrees with the observation that there is no crack opening from the punch side for this material.

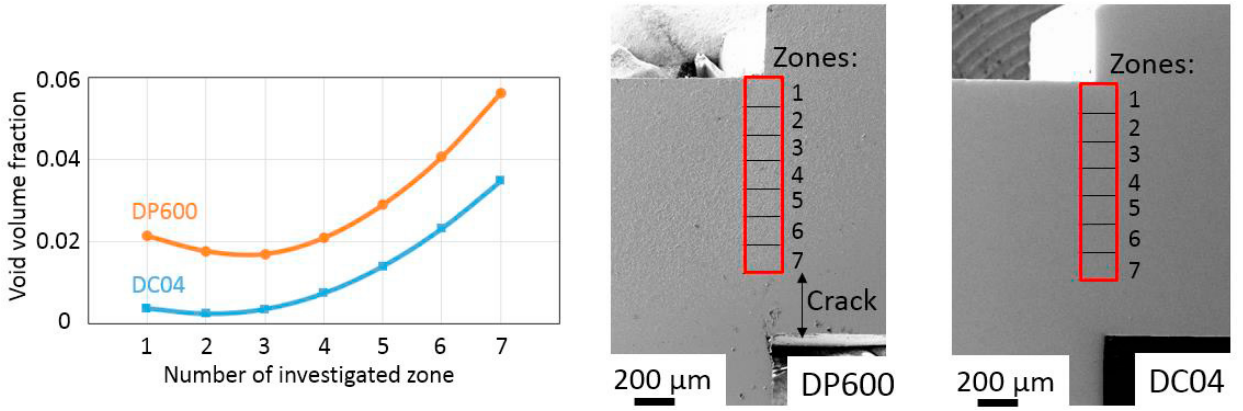

Fig. 6. Void volume fractions at the shearing region and representation of the investigated zones

5. Conclusion

The simulations of the punching experiment using the Gurson model with recent shear extension can predict the crack initiation for the investigated materials. Without consideration of the void growth due to shear stresses, the simulations show postponed cracks which is not fitting with the experiments. The crack initiation for both materials differentiate such that DP600 shows crack opening from both punch and die side of the specimen. That phenomena can be modelled by this model correctly. The micromechanical basis of the Gurson model provides the direct utilization of the micromechanical void events, such as void nucleation, growth and coalescence for the identifications of the model parameter. The extension for the consideration of the shear stresses mainly arises from the physical observations on distortion and interactions of voids with material rotation under shear. The applied stress state dependent function $w(\mathrm{dev}[\mathbf{T}])$ (Eq. 6) distinguishes the triaxial stress states from generalized plane strain states using third invariant of the stress tensor. With scaling parameter k_w, the amount of the void growth can be included phenomenologically. By a coincidence for both materials, the identified k_w from force-displacement curves turned out to be equal to 1. For similar material classes, it might be expected that this value is alike. For this conclusion, more materials from different classes should be investigated.

The sheared surface for both materials shows differences in the proportion of shear and crack surface. Even a secondary shear surface is observed for DP600. This surface characteristics affect the overall punch force drop regime for the specimen. Although the element deletion technique considers the crack opening and corresponding force drop, there are some limitations for the cases where we have secondary shear surfaces. The void volume fraction measurements shows accordance with the crack opening regions. The voidage is increasing at the shearing region. This micromechanical observation highlights the necessity of the void growth under shear stress states. The maximum measured void fractions measured is smaller than the critical void volume fraction threshold value for the element deletion (f_f =0.25). Because of the crack formation during separation, distinguishing the macro-cracks and voids at the sheared surface is not straightforward. Therefore the crack region is excluded from the micromechanical measurements for void volumes. That results in relatively conservative values which include only micro-voids. For initial volume fractions and at the sheared surface for each zone, the measured voidage for the DP600 is higher than DC04. The rapid crack occurrence and growth can be explained with this observation.

Acknowledgements

The authors gratefully acknowledge funding by the German Research Foundation (DFG) within the scope of the Transregional Collaborative Research Centre on sheet-bulk metal forming (SFB/TR 73) in the subproject C4 'Analysis of load history dependent evolution of damage and microstructure for the numerical design of sheet-bulk metal forming processes'.

References

Nahshon, K., Hutchinson, J.W., 2008. Modification of the Gurson Model for shear failure. European Journal of Mechanics - A/Solids 27(1), 1-17.

Atkins, A.G., 1981. Surfaces produced by guillotining Philosophical Magazine 43A, 627–641.

Atkins, A.G., 1980. On cropping and related processes. International Journal of Mechanical Science 22, 215-231.

Martins, P.A.F., Atkins, A.G., 2013. Revisiting the empirical relation for the maximum shearing force using plasticity and ductile fracture mechanics. Journal of Materials Processing Technology 213(9), 1516-1522.

Thipprakmas, S., Jin, M., Tomokazu, K., Katsuhiro, Y., Murakawa, M., 2008. Prediction of Fineblanked surface characteristics using the finite element method (FEM). Journal of Materials Processing Technology 198(1–3), 391-398.

Hambli, R., 2001. Finite element simulation of fine blanking processes using a pressure-dependent damage model. Journal of Materials Processing Technology 116(2–3), 252-264.

Lemaitre, J., 1985. A continuous damage mechanics model for ductile fracture. J. Eng. Mater. Technol. 107, 83-89.

Rachik, M., Roelandt, J.M., Maillard, A., 2003. Numerical Simulation of sheet metal blanking predicting the shape of the cut edge. Key Engineering Materials 233-236, 329-334.

Tvergaard, V., Needleman, A., 1984. Analysis of cup-cone fracture in a round tensile bar. Acta Metallurgica 32(1), 157-169.

Brokken, D., Brekelmans, W.A.M., Baaijens, F.P.T., 1998. Numerical modelling of the metal blanking process. Journal of Materials Processing Technology 83, 192-199.

Komori, K., 2014. Simulation of stationary crack during blanking using node separation method. Procedia Engineering 81, 1102 – 1107.

Gurson, A.L., 1977. Continuum theory of ductile rupture by void nucleation and growth - Part I. Yield criteria and rules for porous ductile media. Journal of Engineering Materials and Technology 99(1), 2-15.

Tvergaard, V., 1981. Influence of voids on shear band instabilities under plane strain conditions. International Journal of Fracture 17(4), 389-407.

Tvergaard, V., 1982. On localization in ductile materials containing spherical voids. International Journal of Fracture 18(4), 237-252.

Soyarslan, C., Faßmann, D., Plugge, B., Isik, K., Kwiatkowski, L., Schaper, M., Brosius, A., Tekkaya, A.E., 2011. An Experimental and Numerical Assessment of Sheet-Bulk Formability of Mild Steel DC04. Journal of Manufacturing Science and Engineering 133(6), 1-9.

Isik, K., Gerstein, G., Clausmeyer, T., Nürnberger, F., Tekkaya, A.E., Maier, H.J., 2016. Evaluation of Void Nucleation and Development during Plastic Deformation of Dual-Phase Steel DP600. Steel research international, doi: 10.1002/srin.201500483.

Gerstein, G., Bruchanov, A.A., Dyachok, D.V., Nürnberger, F. 2016. The effect of texture in modeling deformation processes of bcc steel sheets, Materials Letters 164, 356-359.